We A3 02

Revealing Shallow and Deep Complex Geological Features with FWI - Lessons Learned

N. Chazalnoel (CGG), A. Gomes* (CGG), W. Zhao (CGG), B. Wray (CGG)

Summary

Conventional full waveform inversion (FWI), mostly based on diving waves, has become a standard velocity model building tool. Using a deep water dataset from the Mexican side of the Gulf of Mexico (GoM), we show that FWI can be effective at resolving different types of complex geological features in the shallow overburden. Unfortunately, it is well known that below the diving-wave penetration depth, FWI has to rely solely on reflections. In this case, the velocity update is dominated by high-wavenumber components and the inversion dependence on the accuracy of the density model increases. However, we show that the reflections can still help solve for the low wavenumbers of the velocity model when different components of the FWI gradient are used separately for reflection-wave-based full waveform inversion (RFWI). This allowed reflection data to improve the velocity model at a geologically challenging location within our GoM project area, namely where traditional ray-based tomography failed and the depth of the required updates exceeded the diving-wave penetration. We discuss the lessons learned for RFWI from this example.

Introduction

Conventional full waveform inversion, mostly based on diving waves and referred to as FWI in this paper, has become a standard velocity model building tool. We use a large deep water survey on the Mexican side of the Gulf of Mexico (GoM) to show that FWI is able to solve for several types of difficult shallow geological velocity structures. We then alternate between density and velocity updates, using the high-wavenumber and low-wavenumber components of the FWI gradient, respectively, to show that reflection-wave-based full waveform inversion (RFWI) can also help solve for deep, complex geological features. Finally, we discuss our observations on the requirements and limitations of this technique.

Geological setting

The area of interest is located on the Mexican side of the prolific Perdido fold belt of the GoM. The water bottom depth ranges from 200 m to 3500 m. Major features include salt walls, pinched diapirs and several vast salt nappes flowing from north-west to south-east. Ahead of the nappes, compression-driven, advancing salt formed overturned beds, thrusts, and highly folded sediments sometimes lying over thick layers of mobile shale. Above the nappes, we find rafted carbonate carapaces sitting on top of the salt and extensional features where salt diapirism created large normal faults and grabens. In such a geologically complex setting, high-resolution ray-based tomography methods struggle to capture the details of the rapid changes in velocity.

Conventional diving-wave-based full waveform inversion

We performed FWI (Tarantola, 1984), which has shown its ability to provide high-resolution velocity models (Sirgue et al., 2010; Warner et al., 2013), using flat cable wide-azimuth (WAZ) acquisition data with maximum offset of 8.1 km along the cables and 4.2 km across the cables. We ran FWI from 4 to 7 Hz with minimal noise attenuation applied to the input data. We extracted the wavelet from the data, and the initial model was obtained from a few iterations of ray-based reflection tomography followed by interpretation of simplified salt bodies built with one top and one base surfaces.
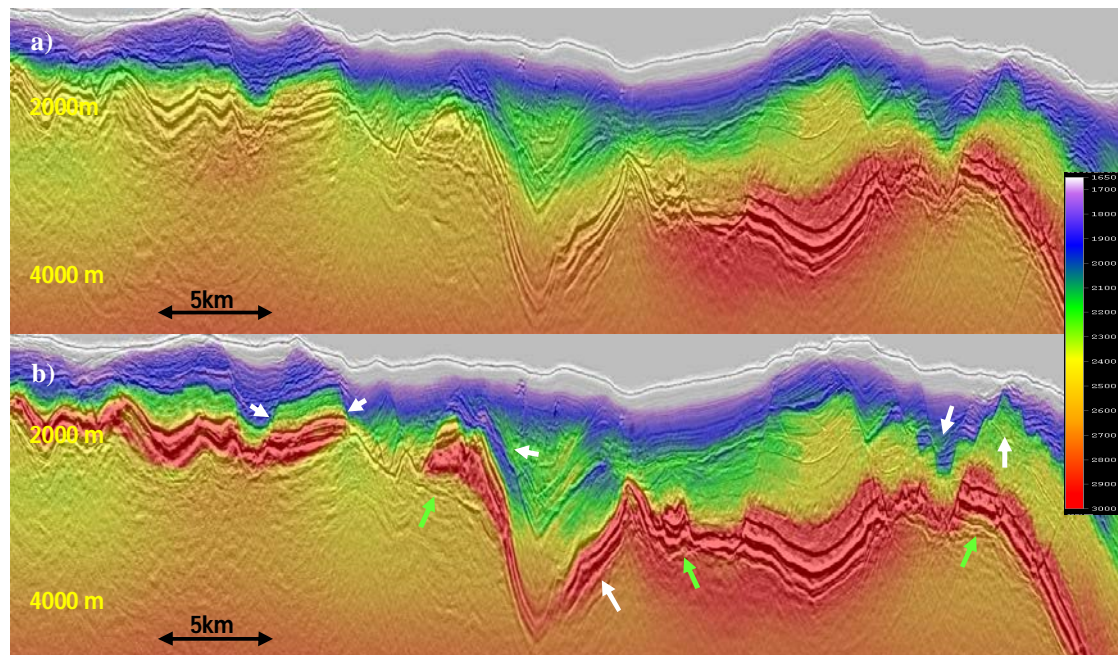

Figure 1 *Depth section in the area above salt with the velocity model overlaid on Kirchhoff migration stack for: a) initial model, and b) FWI updated model. White arrows indicate places where the FWI velocity model is improved. Green arrows point to improvements in the top of salt image.*

FWI accurately detected details of the velocity in the shallow overburden unresolved by tomography. Also, the FWI velocity model became more conformal to the seismic units and structural truncations. It shows good correlation with the stratigraphy, i.e., fast in the carbonates and slow in the shales. Low-velocity anomalies are possible indications of gas or fluids. Above salt (Figure 1), the velocities from different layers are well separated in the FWI model, including in the different fault blocks of the graben areas and in the rafted carbonate carapaces. The FWI model has also improved focusing in the migrated image. In particular, we observe better focused graben faults, and a stronger, more coherent top of salt under the carbonates. Similarly, in the pressure ridge ahead of the salt, FWI was able to detect details of the different velocities of the thrust blocks and overturned beds (Figure 2).

We found FWI to be a robust tool for obtaining a high-resolution velocity model in the various complex geologic settings found in the overburden of our large area. However, because of the limited penetration of the diving waves, the benefits of FWI are often restricted to no more than a couple of kilometers below the water bottom. Below that, it has to rely on reflections and is limited by two main requirements that are difficult to ensure over a large area. First, the update from reflections is dominated by high-wavenumber components of the velocity (Mora, 1989), which often have little effect on the kinematics of the migration. This means that FWI requires a good starting model; otherwise, sharp boundaries can be placed in the wrong locations. Second, FWI becomes more dependent on the quality of the density model used in the inversion (Guitton, 2014).
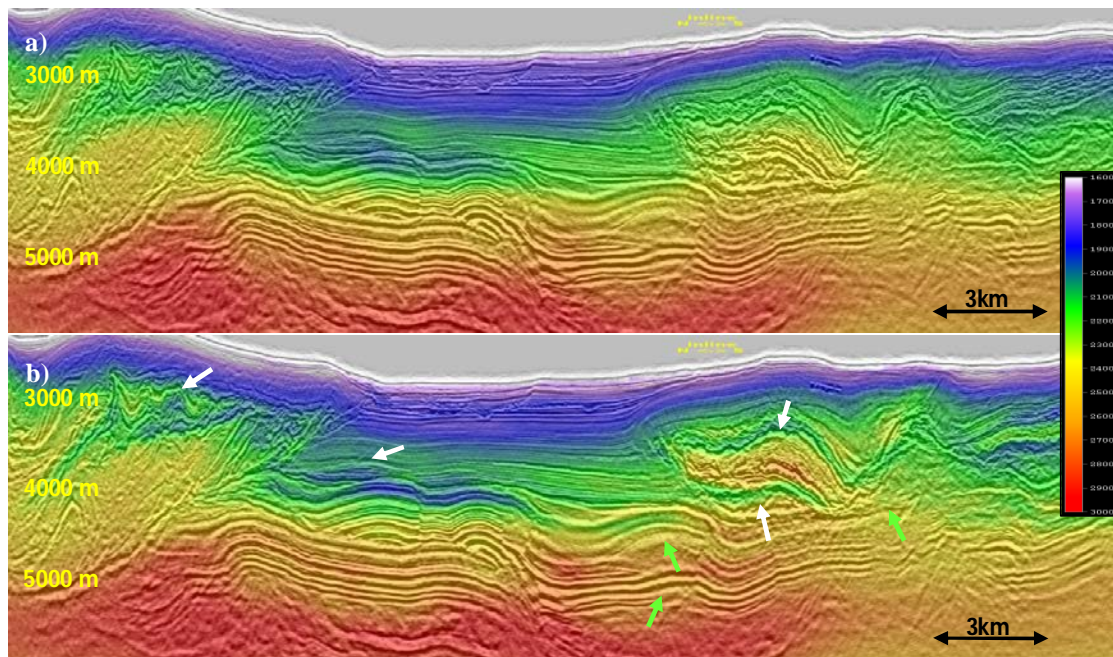

Figure 2 *Depth section in the area ahead of the salt nappes with the velocity model overlaid on Kirchhoff stack for: a) initial model, and b) FWI updated model. White arrows indicate places where the FWI velocity model is improved. Green arrows point to improvements in the image.*

Reflection-based full waveform inversion

To overcome these issues, for our RFWI we separate the low- and high-wavenumber components of the FWI gradient (Tang et al., 2013). FWI generates a low-wavenumber update when incident and scattered wavefields travel through the model in the same direction (Mora, 1989), i.e., backscattered energy of deep reflections. By decomposing the wavefields based on their directions of propagation, it is therefore possible to separate the high- and low-wavenumber components of the FWI gradient.
Sun et al. (2016) use a migration or least-squares migration to first generate a reflectivity model and then follow with Born modelling to update the low-wavenumber components of the velocity by wavefield decomposition. Similarly, Irabor and Warner (2016) use gradient decomposition based on

the direction of propagation of the wavefields to first update high-wavenumber components of the velocity in order to generate the reflectivity used in the next iteration to update the low-wavenumber components of the velocity. The first high-wavenumber update is later removed, preserving only the low-wavenumber velocity update. In our RFWI, we use these terms alternately to update density and velocity, respectively. The density update iteration introduces the deep reflectors needed in the next iteration for generation of the backscattered energy required for the low-wavenumber velocity update. Updating density in the former iteration has the advantage of not changing the kinematics of the process; hence it can tolerate some inaccuracies in the estimated density values, while the traveltime fidelity of the current model is honored in the latter velocity update iteration.
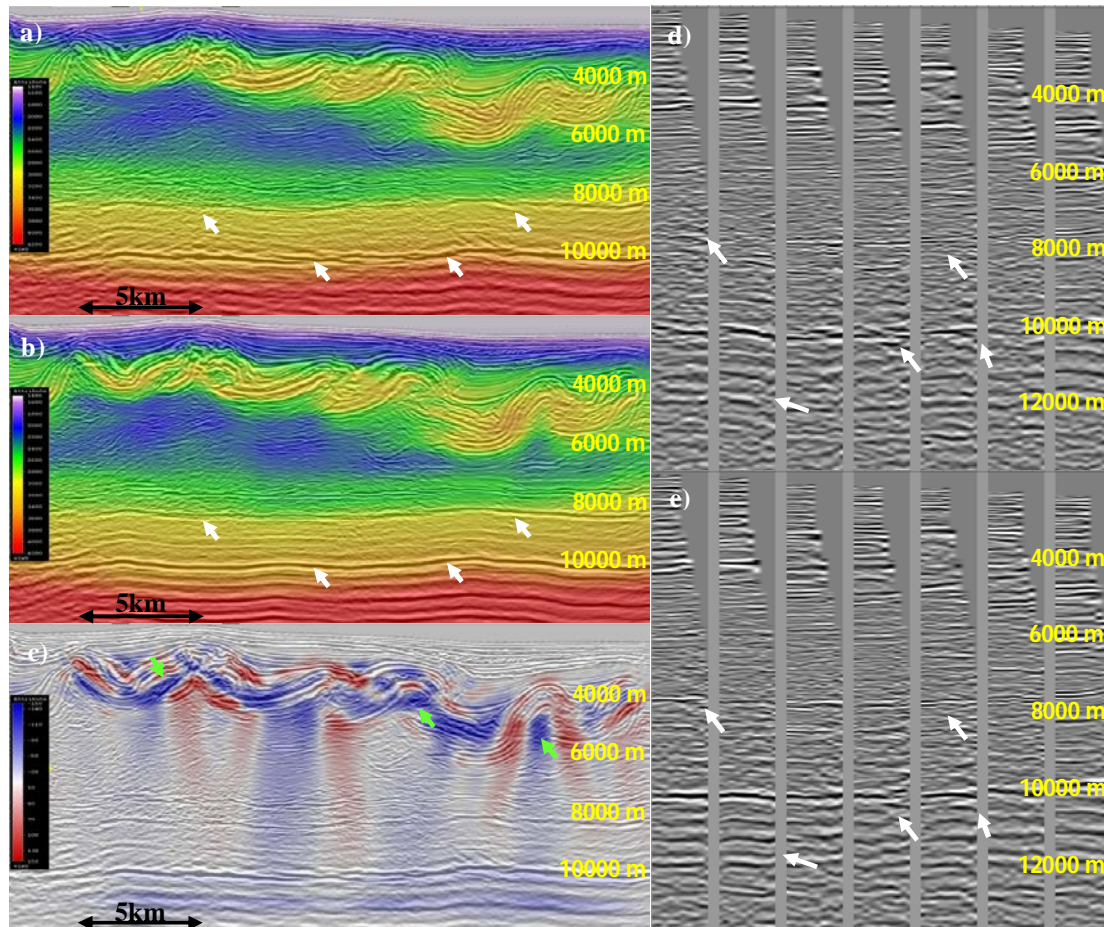

Figure 3 *Depth section with the velocity model overlaid on RTM stack for: a) initial model, b) RFWI updated model, and c) RFWI velocity perturbation. RTM SOGs over the same line from: d) initial model, and e) RFWI updated model. White arrows indicate image improvements at the Wilcox and Cretaceous events on the stack and improvements in coherency and flatness on the SOGs. Green arrows point to where lower velocities indicate embedded shale towards the crest of the folds.*

Using this strategy, we applied RFWI from 4 to 7 Hz in the compression area ahead of the salt, where we find deeper folds, which were barely penetrated by the diving waves, sitting on top of thick mobile shales. We used the same WAZ data as for FWI but after source and receiver deghosting, zero-phasing, and SRME demultiple. Using these further processed data proved beneficial (although the reasons for this are still under investigation). We used velocity scans and ray-based tomography after the previous FWI to generate the initial velocity model. The complexity of the folds combined with the low reflectivity of the shales make it very difficult for traditional velocity update methods to provide a viable solution. RFWI is, on the other hand, able to improve both the velocity model and the corresponding image down to a depth of more than 10 km. This can be seen clearly from the

improved continuity of the deeper Wilcox and Cretaceous events (Figures 3a-b). The velocity perturbation from RFWI (Figure 3c) indicates reliably updated complex areas where the underlying shales are thrusted within the folds. It also shows the vertical nature of the update, and therefore its lack of vertical resolution. This might be an intrinsic limitation of RFWI due to limited incidence angles of deeper reflections. RTM surface offset gathers (SOGs) confirm through event coherency and flatness improvements that the update, although not perfect, provides a clear uplift (Figures 3d-e).

Conclusion and discussion

We have shown that FWI and RFWI can be used to resolve both shallow and deep complex geological features. Conventional FWI is able to provide a high-resolution velocity model and improve the image in the different geological settings of our area. The main drawback of conventional FWI is its reliance on diving-wave penetration, which limits its updates to the shallow overburden. In our example, RFWI is able to update the low-wavenumber component of the velocity model and the image much deeper than the diving-wave penetration.

It is worth noting that our example was favorable for RFWI since: (1) it used WAZ data, which provides good illumination coverage, and (2) in our area, the complex velocity zones of the folds and mobile shales are situated above strong, deep events (Top Wilcox and Cretaceous). Even with that, the velocity perturbation and the RTM SOGs with the updated model show that RFWI still lacks vertical resolution and the output model is not yet perfect. From applying it on a large area, we also noticed that RFWI does not always show much improvement in places where the initial image is poor, possibly because the starting model is too inaccurate. Nonetheless, the large global improvement obtained by our RFWI shows that this technique is worth understanding and improving further, as it could become a valuable tool for updating the deeper section of velocity models.

Acknowledgements

References

Guitton, A. [2014] On the velocity-density ambiguity in acoustic full-waveform inversion. *76th EAGE Conference & Exhibition,* Extended Abstracts, We E106 03.

Irabor, K. and Warner, M. [2016] Reflection FWI. *SEG Technical Program Expanded Abstracts,* 1136-1140.

Mora, P. [1989] Inversion = migration + tomography. *Geophysics,* **54**(12), 1575-1586.

Sirgue, L., Barkved, O.J., Dellinger, J., Etgen, J., Albertin, U. and Kommedal J.H. [2010] Full waveform inversion: the next leap forward in imaging at Valhall. *First Break,* **28**(4), 65-70.

Sun, D., Jiao, K., Cheng, X. and Vigh, D. [2016] Reflection based waveform inversion. *SEG Technical Program Expanded Abstracts*, 1151-1156.

Tang, Y., Lee, S., Baumstein, A. and Hinkley, D. [2013] Tomography enhanced full wavefield inversion. *SEG Technical Program Expanded Abstracts*, 1037-1041.

Tarantola, A. [1984] Inversion of seismic reflection data in the acoustic approximation. *Geophysics,* **49**, 1259-1266.

Warner, M., Ratcliffe, A., Nangoo, T., Morgan, J., Umpleby, A., Shah, N., Vinje, V., Stekl, I., Guasch, L., Win, C., Conroy, G. and Bertrand, A. [2013] Anisotropic 3D full-waveform inversion. *Geophysics,* **78**(2), 59-80.